

# Modulation of Metallophilic Bonds: Solvent-Induced Isomerization and Luminescence Vapochromism of a Polymorphic Au–Cu Cluster

Igor O. Koshevoy,<sup>\*,†</sup> Yuh-Chia Chang,<sup>‡</sup> Antti J. Karttunen,<sup>†</sup> Matti Haukka,<sup>†</sup> Tapani Pakkanen,<sup>†</sup> and Pi-Tai Chou<sup>\*,‡</sup>

<sup>†</sup>Department of Chemistry, University of Eastern Finland, Joensuu 80101, Finland

<sup>‡</sup>Department of Chemistry, National Taiwan University, Taipei 106, Taiwan

## S Supporting Information

**ABSTRACT:** We report a homoleptic Au–Cu alkynyl cluster that represents an unexplored class of luminescent materials with stimuli-responsive photophysical properties. The bimetallic complex formulated as  $[\text{Au}_2\text{Cu}_2(\text{C}_2\text{OHC}_5\text{H}_8)_4]_n$  efficiently self-assembles from  $\text{Au}(\text{SC}_4\text{H}_8)\text{Cl}$ ,  $\text{Cu}(\text{NCMe})_4\text{PF}_6$ , and 1-ethynylcyclopentanol in the presence of  $\text{NEt}_3$ . This compound shows remarkably diverse polymorphism arising from the modulation of metallophilic interactions by organic solvents. Four crystalline forms, obtained from methanol (**1a**); ethanol, acetone, or chloroform (**1b**); toluene (**1c**); and diethyl ether or ethyl acetate (**1d**), demonstrate different photoluminescent characteristics. The solid-state quantum yields of phosphorescence ( $\Phi$ ) vary from 0.1% (**1a**) to 25% (**1d**), depending on the character of intermetallic bonding. The structures of **1b–d** were determined by single-crystal X-ray diffraction. The ethanol (**1b**,  $\Phi = 2\%$ ) and toluene (**1c**,  $\Phi = 10\%$ ) solvates of  $[\text{Au}_2\text{Cu}_2(\text{C}_2\text{OHC}_5\text{H}_8)_4]_n$  adopt octanuclear isomeric structures ( $n = 2$ ), while **1d** ( $\Phi = 25\%$ ) is a solvent-free chain polymer built from two types of  $\text{Au}_4\text{Cu}_4$  units. Electronic structure calculations show that the dramatic enhancement of the emission intensity is correlated with the increasing role of metal–metal bonding. The latter makes the emission progressively more metal-centered in the order **1b** < **1c** < **1d**. The metallophilic contacts in **1a–d** show high sensitivity to the vapors of certain solvents, which effectively induce unusual solid-state isomerization and switching of the absorption and luminescence properties via non-covalent interactions. The reported polymorphic material is the first example of a gold(I) alkynyl compound demonstrating vapochromic behavior.

Non-covalent interactions between  $d^{10}$  ions of copper subgroup metals (metallophilicity) play a fundamentally important role in the very diverse and fascinating coordination chemistry of these elements, often governing the formation of various molecular or polymeric assemblies of a multimetallic nature.<sup>1</sup> Numerous coinage-metal complexes possessing effective metal–metal contacts demonstrate an attractively wide range of light-emissive properties, including tunable photoluminescence<sup>2</sup> and its mechano-,<sup>3</sup> tribo-,<sup>4</sup> solvo-,<sup>5</sup> or vapochromic alteration.<sup>6</sup> The vapochromic phenomenon has been actively investigated recently because of the promising

potential of stimuli-responsive organopolymetallic materials for selective and easy-to-detect sensing of volatile organic compounds (VOCs).

The changes in the observed optical properties are generally attributed to the modulation of inter- or intramolecular metal–metal bonds<sup>3,4,6b,7</sup> or metal–solvent bonds<sup>8</sup> and, very rarely, to an isomerization due to the insertion of VOC molecules into the crystal lattice.<sup>9</sup> Among metallophilic interactions involving Cu, Ag, and Au ions, which are susceptible to the influence of external factors (heat, mechanical force, guest molecule, etc.), most of the research has been dedicated to Au–Au,<sup>3,4,6b,10</sup> Au–Ti,<sup>6a,8a</sup> and Au–Ag contacts.<sup>8b,11</sup> Materials that contain Au–Cu bonds and demonstrate switching of color and/or luminescence characteristics upon application of a stimulus remain extremely scarce.<sup>5c,7</sup> Moreover, to the best of our knowledge, vapor-responsive behavior of the alkynyl complexes of coinage metals has never been described, despite a very large amount of experimental work being devoted to this versatile class of compounds.<sup>12</sup>

We recently reported a family of Au–Cu alkynyl diphosphine complexes bearing hydroxoaliphatic alkynes, where the tetranuclear clusters  $\text{Au}_2\text{Cu}_2(\text{C}_2\text{R})_4$  were stabilized by external gold–diphosphine fragments.<sup>13</sup> This work, together with that of Eisenberg, in which a similar compound,  $[\text{Au}_2\text{Cu}_2(\text{C}_2\text{R})_4]_2$  ( $\text{R} = \text{estradiol}$ ), was isolated,<sup>14</sup> inspired us to investigate the possibility of preparing other alkynyl Au–Cu homoleptic clusters based on a tetranuclear core, a general motif that serves as a building block for an important family of luminescent materials,  $[\text{Au}_2\text{Ag}_2(\text{C}_6\text{Hal}_5)_4]_n$  ( $\text{Hal} = \text{halide}$ ), having intriguing vapochromic properties.<sup>6b,8b,11</sup>

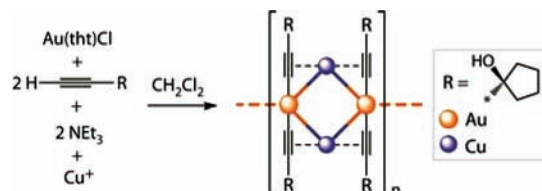
The reaction of  $\text{Au}(\text{tht})\text{Cl}$  ( $\text{tht} = \text{tetrahydrothiophene}$ ) with 1-ethynylcyclopentanol in the presence of  $\text{NEt}_3$  and subsequent addition of  $\text{Cu}(\text{NCMe})_4\text{PF}_6$  resulted in the formation of a novel complex formulated as  $[\text{Au}_2\text{Cu}_2(\text{C}_2\text{OHC}_5\text{H}_8)_4]_n$  (Scheme 1), which was isolated as nearly colorless micro-needles after the reaction mixture was treated with methanol (**1a**).

This synthetic approach is different from that used recently<sup>14</sup> for the preparation of the pentanuclear anionic cluster  $[\text{Au}_3\text{Cu}_2(\text{C}_2\text{OHC}_5\text{H}_8)_6]^-$  and allows for the preparation of the neutral species. The crystals obtained from methanol were not suitable for X-ray diffraction analysis. Recrystallization of **1**

Received: February 28, 2012

Published: April 2, 2012

## Scheme 1. Synthesis of Complex 1



from ethanol gave yellow block crystals of form **1b**. The structure (Figure 1 left) contains an octanuclear cluster,  $\text{Au}_4\text{Cu}_4(\text{C}_2\text{OHC}_5\text{H}_8)_8$ , that is formed via fusion of the  $\{\text{Au}_2\text{Cu}_2\}$  units and redistribution of the copper ions. The resulting staggered arrangement of Cu atoms decreases the number of effective metal–metal contacts within the metal framework. The cluster core is held together by the metal–metal interactions and bridging  $\pi\text{-C}\equiv\text{C}$  coordination of the alkynyl ligands. Additionally, it is stabilized by  $\text{O}\cdots\text{H}\cdots\text{O}$  hydrogen bonding between the hydroxylic groups of the alkynyl ligands. The  $\text{Cu}\cdots\text{Au}$  bonding contacts in the molecule of **1b** range from 2.899 to 2.955 Å and are not exceptional [see Table S2 in the Supporting Information (SI) for the selected bond distances].<sup>13,14</sup> Two gold atoms, Au(3) and Au(1), are only slightly involved in the formation of the cluster core, as the distances to the adjacent metal ions exceed the sums of the van der Waals radii (3.06 Å for Au–Cu and 3.32 Å for Au–Au). The Au(2)–Au(4) distance (3.194 Å) indicates the presence of an effective aurophilic contact. The same yellow form **1b** crystallized when acetone or  $\text{CHCl}_3$  was used as the solvent.

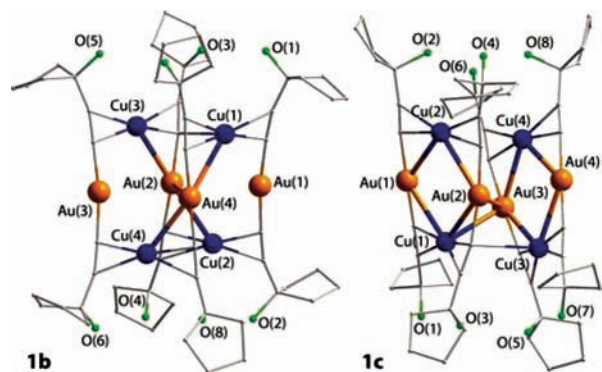


**Figure 1.** Molecular views of the forms (left) **1b** and (right) **1c** (one of two identical molecules in the asymmetric unit of **1c** is shown).

Recrystallization of **1** from toluene gave colorless block crystals of **1c** (Figure 1 right), which has the same composition as **1b** but differs in the distribution of the copper centers. It consists of two roughly planar  $\{\text{Au}_2\text{Cu}_2\}$  fragments linked together via short Au–Au and Au–Cu contacts. All of the metal ions in **1c** participate in metallophilic interactions. The Au–Cu distances in **1c** (2.942–2.998 Å) and the Au–Au contacts (3.319 and 3.287 Å) observed in both independent molecules in the asymmetric unit are slightly longer than those found in **1b**. The unit cells of **1b** and **1c** contain ethanol and toluene solvent molecules, respectively, which are not bound to the metal clusters, except for some  $\text{O}\cdots\text{H}\cdots\text{O}$  hydrogen bonding in the case of **1b**.

Remarkably, crystallization of **1** from ethyl acetate or diethyl ether gave the bright-orange, solvent-free modification **1d** (Figure 2). The solid-state structure of this form shows a

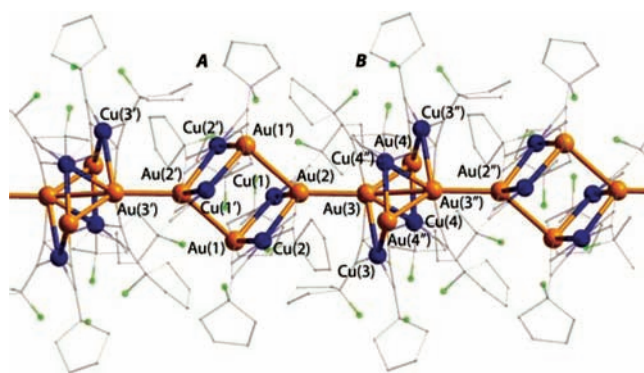


**Figure 2.** Molecular view of the polymeric form **1d**. The  $\{\text{Au}_4\text{Cu}_4\}$  blocks A and B are independently disordered; only one of the possible conformations is shown. Symmetry transformations used to generate equivalent atoms: (')  $1 - x, 1 - y, -z$ ; (")  $2 - x, 1 - y, -z$ .

polymeric chain composed of two types of octanuclear  $\text{Au}_4\text{Cu}_4(\text{C}_2\text{OHC}_5\text{H}_8)_8$  clusters (A and B). These two units are connected to each other by the Au(2)–Au(3) bond (3.024 Å), which is the shortest aurophilic contact within this series of isomers.

The  $\{\text{Au}_4\text{Cu}_4\}$  building blocks A and B in **1d** are constructed from the tetranuclear  $\{\text{Au}_2\text{Cu}_2\}$  units in a similar way as in form **1c**. Thus, the  $\{\text{Au}_4\text{Cu}_4\}$  cluster of type A adopts a prismatic (nearly cubic) structure, where two  $\{\text{Au}_2\text{Cu}_2\}$  rhombs are linked via Au(1)–Au(2') interactions (3.264 Å). The B-type  $\{\text{Au}_4\text{Cu}_4\}$  unit represents a parallelepiped with a considerably shorter distance between the  $\{\text{Au}_2\text{Cu}_2\}$  planes (2.320 Å vs 3.370 Å in the A-type unit).

Form **1a** displays very weak yellow luminescence in the solid state. As seen by the naked eye (Figure 3A, top), its congener **1b** exhibits a slight increase in emission intensity with a very

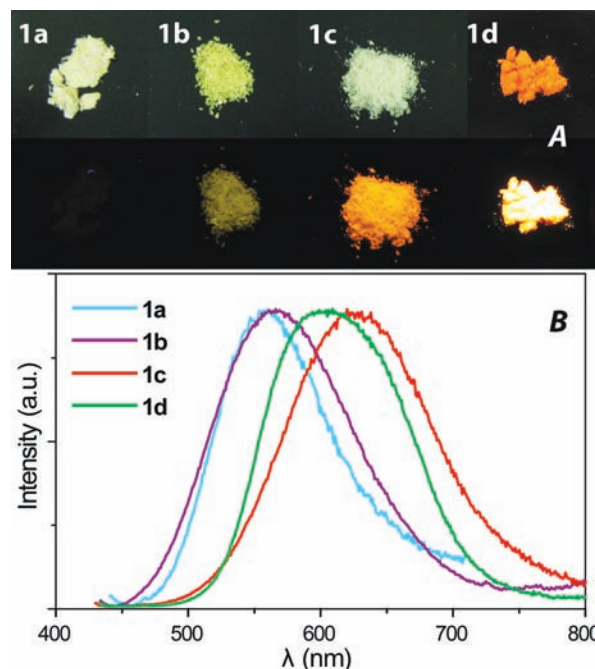


**Figure 3.** (A) Appearance of **1a–d** under ambient light (top) and under UV excitation (bottom,  $\lambda_{\text{exc}} = 365$  nm). (B) Emission spectra (each normalized to the intensity at the peak wavelength) of **1a–d** in the crystalline form.

similar peak wavelength (Figure 3B, bottom). The forms **1c** and **1d** demonstrate a bathochromic shift of the emission profile, accompanied by a significant increase in the emission intensity.

Table 1 lists the photophysical data (emission peak wavelength, quantum yield, and decay dynamics) for the complexes **1a–d** in the solid state at 298 K. The quantum yields were found to increase in the order **1a** ( $<0.001$ )  $<$  **1b** (0.02)  $<$  **1c** (0.10)  $<$  **1d** (0.25). The radiative lifetimes were all measured to be  $>10^{-6}$  s, confirming their phosphorescence origin. Interestingly, as shown in Table 1, the radiative decay constant ( $k_r$ ) also reveals a trend of **1a**  $<$  **1b**  $<$  **1c**  $\ll$  **1d**.

**Table 1. Photophysical Properties of Complexes 1a–d in the Solid State at 298 K**

	$\lambda_{\max}$ (nm)	$\Phi^a$	$\tau_{\text{obs}}$ ( $\mu\text{s}$ )	$k_r$ ( $\text{s}^{-1}$ )	$k_{\text{nr}}$ ( $\text{s}^{-1}$ )	$\tau_{\text{rad}}$ ( $\mu\text{s}$ )
<b>1a</b>	582	0.001	0.4	$2.5 \cdot 10^3$	$2.5 \cdot 10^6$	400
<b>1b</b>	566	0.02	7.6	$2.6 \cdot 10^3$	$1.3 \cdot 10^5$	380
<b>1c</b>	620	0.10	17.9	$5.6 \cdot 10^3$	$5.0 \cdot 10^4$	179
<b>1d</b>	609	0.25	1.4	$1.8 \cdot 10^5$	$5.4 \cdot 10^5$	6

<sup>a</sup>Determined with a calibrated integrating sphere system (avg error  $\approx$  2%).

We further elucidated the above photophysical characteristics of the complexes **1b–d** by means of density functional theory calculations (PBE0-DFT; see the SI for computational details). The transition densities for the lowest-energy singlet excitation  $S_0 \rightarrow S_1$  are shown in Figure 4. For **1b**, the transition density is mostly centered on the alkynyl ligands and Cu atoms, while the gold atoms play a minor role. In **1c**, the contribution of the Au atoms becomes more significant, and the excitation is generally more metal-centered. In the case of **1d**, the excitation is almost completely centered on the chain of Au atoms in the polymeric structure. The increasing importance of the gold(I) ions in moving from **1b** to **1d** is in accordance with the experimental observation of the trend of increasing radiative decay rate constant. The results demonstrate the effect of the spin–orbit coupling arising from the heavy Au atoms, which enhances the singlet–triplet mixing and hence the  $T_1 \rightarrow S_0$  transition. In the case of the polymer **1d**, the relay of the metal–metal arrangement may lead to further enhancement, giving an anomalous increase in the radiative decay rate constant (see  $k_r$  in Table 1). Accordingly, despite the similar magnitudes of the

radiationless decay rate constants ( $k_{\text{nr}}$ ) for **1b–d** (Table 1), a much higher emission yield (25%) is observed for polymer **1d**.

As form **1d** is solvent-free, we decided to test its behavior toward the vapors of different solvents (VOCs). Indeed, exposure of **1d** to methanol vapor at room temperature resulted in fast decolorization of the solid and a dramatic drop in the emission intensity that presumably points to the transformation of **1d** into **1a**. Interestingly, this isomerization was reversible, as treatment of **1a** with diethyl ether or ethyl acetate vapors led to the appearance of the orange-yellow color and intense emission corresponding to the starting material **1d** (Figure S1 in the SI). Similar to **1d**, forms **1b** and **1c** demonstrated sensitivity to methanol vapor, which caused a significant decrease in photoemission and a shift to the yellow region in the case of **1c**. The modifications **1b** and **1c** were not responsive to diethyl ether or ethyl acetate solvents, but they were quickly converted into **1d** thermally at ca. 135 and 115 °C, respectively (Figure S2). The transformation of **1b** to **1d** appeared to be accompanied by some minor degradation. The **1b**  $\rightarrow$  **1d** isomerization occurs at a higher temperature than the **1c**  $\rightarrow$  **1d** transition presumably because of the inevitable solid-state redistribution of the copper ions. This process is required for **1b** in order to provide the planar  $\{\text{Au}_2\text{Cu}_2\}$  building blocks forming the polymeric chain of **1d**. Form **1c** already contains  $\{\text{Au}_4\text{Cu}_4\}$  octanuclear units similar to those found in the structure of **1d**. Thus, substantial rearrangements during the **1c**  $\rightarrow$  **1d** transformation are not required, and the transition has a lower energy barrier. The latter probably corresponds mainly to thermal removal of the toluene crystallization molecules. The thermal transition **1a**  $\rightarrow$  **1d** could not be achieved; instead heating of **1a** resulted in decomposition of **1a** only. A summary of the diverse transformations observed is given in Scheme 2.

**Scheme 2. Summary of the Observed Interconversions among 1a–d (Solvents Indicate Their Vapors)**

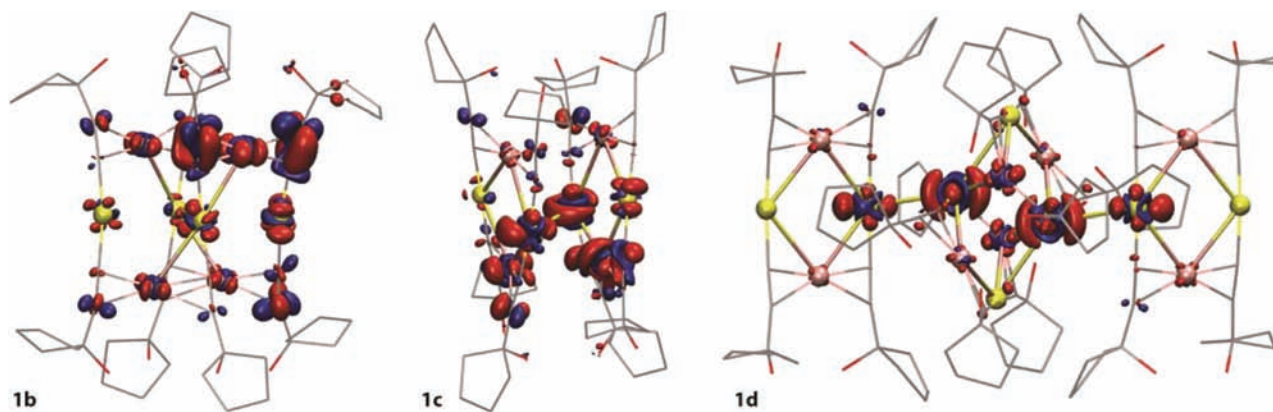
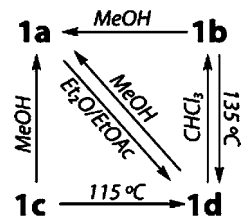


**Figure 4.** PBE0-DFT transition densities for the lowest-energy singlet excitations of **1b–d** (density isovalue 0.002 au). During the electronic transition, the electron density increases in the blue areas and decreases in the red areas. H atoms have been omitted for clarity.



In summary, we have reported a novel luminescent Au–Cu homoleptic alkynyl cluster showing diverse polymorphism, which is directed by the solvent medium used. The four crystalline forms discovered here exhibit different photoluminescence behavior, showing quantum yields from 0.1 to 25% depending on the character of the metallophilic bonding. For the first time, vapochromic behavior of a gold(I) alkynyl compound has been described. This phenomenon, originating from the effective modulation of the intermetallic contacts, results in unusual solid-state isomerization caused by the vapors of certain organic solvents via non-covalent interactions.

## ■ ASSOCIATED CONTENT

### 📄 Supporting Information

Experimental details, X-ray crystallographic data (CIF) for **1b–1d**, and Cartesian coordinates of the structures of **1b–1d**. This material is available free of charge via the Internet at <http://pubs.acs.org>.

## ■ AUTHOR INFORMATION

### Corresponding Author

igor.koshevoy@uef.fi; chop@ntu.edu.tw

### Notes

The authors declare no competing financial interest.

## ■ ACKNOWLEDGMENTS

We thank University of Eastern Finland (Spearhead Project and Finnish–Russian Collaborative Project) and the Academy of Finland (Grant 138560/2010 to A.J.K.) for financial support.

## ■ REFERENCES

- (1) (a) Silvestru, C. Gold–Heterometal Interactions and Bonds. In *Modern Supramolecular Gold Chemistry*; Laguna, A., Ed.; Wiley-VCH: Weinheim, Germany, 2008; pp 181–295. (b) Puddephatt, R. J. *Chem. Soc. Rev.* **2008**, *37*, 2012–2027. (c) Schmidbaur, H.; Schier, A. *Chem. Soc. Rev.* **2012**, *41*, 370–412.
- (2) (a) Che, C.-M.; Lai, S.-W. Luminescence and Photophysics of Gold Complexes. In *Gold Chemistry*; Mohr, F., Ed.; Wiley-VCH: Weinheim, Germany, 2009; pp 249–282. (b) López-de-Luzuriaga, J. M., Luminescence of Supramolecular Gold-Containing Materials. In *Modern Supramolecular Gold Chemistry*; Laguna, A., Ed.; Wiley-VCH: Weinheim, Germany, 2008; pp 347–402. (c) He, X.; Yam, V. W.-W. *Coord. Chem. Rev.* **2011**, *255*, 2111–2123. (d) Yam, V. W.-W.; Wong, K. M.-C. *Chem. Commun.* **2011**, *47*, 11579–11592.
- (3) Ito, H.; Saito, T.; Oshima, N.; Kitamura, N.; Ishizaka, S.; Hinatsu, Y.; Wakeshima, M.; Kato, M.; Tsuge, K.; Sawamura, M. *J. Am. Chem. Soc.* **2008**, *130*, 10044–10045.
- (4) Lee, Y.-A.; Eisenberg, R. *J. Am. Chem. Soc.* **2003**, *125*, 7778–7779.
- (5) (a) Vickery, J. C.; Olmstead, M. M.; Fung, E. Y.; Balch, A. L. *Angew. Chem., Int. Ed. Engl.* **1997**, *36*, 1179–1181. (b) Fung, E. Y.; Olmstead, M. M.; Vickery, J. C.; Balch, A. L. *Coord. Chem. Rev.* **1998**, *171*, 151–159. (c) Chen, K.; Strasser, C. E.; Schmitt, J. C.; Shearer, J.; Catalano, V. J. *Inorg. Chem.* **2012**, *51*, 1207–1209.
- (6) (a) Fernández, E. J.; López-de-Luzuriaga, J. M.; Olmos, M. E.; Monge, M.; Pérez, J.; Laguna, A.; Mohamed, A. A.; Fackler, J. P., Jr. *J. Am. Chem. Soc.* **2003**, *125*, 2022–2023. (b) Lasanta, T.; Olmos, M. E.; Laguna, A.; López-de-Luzuriaga, J. M.; Naumov, P. *J. Am. Chem. Soc.* **2011**, *133*, 16358–16361. (c) Lim, S. H.; Olmstead, M. M.; Balch, A. L. *J. Am. Chem. Soc.* **2011**, *133*, 10229–10238.
- (7) Strasser, C. E.; Catalano, V. J. *J. Am. Chem. Soc.* **2010**, *132*, 10009–10011.
- (8) (a) Fernández, E. J.; López-de-Luzuriaga, J. M.; Monge, M.; Montiel, M.; Olmos, M. E.; Pérez, J.; Laguna, A.; Mendizabal, F.; Mohamed, A. A.; Fackler, J. P., Jr. *Inorg. Chem.* **2004**, *43*, 3573–3581.

- (b) Laguna, A.; Lasanta, T.; López-de-Luzuriaga, J. M.; Monge, M.; Naumov, P.; Olmos, M. E. *J. Am. Chem. Soc.* **2010**, *132*, 456–457.
- (9) Cariati, E.; Bu, X.; Ford, P. C. *Chem. Mater.* **2000**, *12*, 3385–3391.
- (10) He, X.; Lam, W. H.; Zhu, N.; Yam, V. W.-W. *Chem.—Eur. J.* **2009**, *15*, 8842–8851.
- (11) Fernández, E. J.; López-de-Luzuriaga, J. M.; Monge, M.; Olmos, M. E.; Puellas, R. C.; Laguna, A.; Mohamed, A. A.; Fackler, J. P., Jr. *Inorg. Chem.* **2008**, *47*, 8069–8076.
- (12) (a) Abu-Salah, O. M. *J. Organomet. Chem.* **1998**, *565*, 211–216. (b) Lima, J. C.; Rodriguez, L. *Chem. Soc. Rev.* **2011**, *40*, 5442–5456.
- (13) Koshevoy, I. O.; Lin, C.-L.; Karttunen, A. J.; Jänis, J.; Haukka, M.; Tunik, S. P.; Chou, P.-T.; Pakkanen, T. A. *Chem.—Eur. J.* **2011**, *17*, 11456–11466.
- (14) Manbeck, G. F.; Brennessel, W. W.; Stockland, R. A., Jr.; Eisenberg, R. *J. Am. Chem. Soc.* **2010**, *132*, 12307–12318.